THE ASTROPHYSICAL JOURNAL, 341:890–900, 1989 June 15

STIMULATED EMISSION OF CARBON RECOMBINATION LINES FROM COLD CLOUDS IN THE DIRECTION OF CASSIOPEIA A

H. E. PAYNE
National Radio Astronomy Observatory
K. R. ANANTHARAMAIAH[1]
National Radio Astronomy Observatory, Very Large Array
AND
W. C. ERICKSON
Astronomy Program, University of Maryland
Received 1988 April 25; accepted 1988 December 1

ABSTRACT

We report observations providing direct evidence for stimulated emission of carbon recombination lines in the direction of Cas A. In observations made at 10 frequencies in the range 34 MHz–325 MHz, the recombination lines were detected in absorption below 115 MHz and in emission above 200 MHz as expected from simple physical considerations of the level populations in high quantum number states. As the brightness temperature of Cas A is very much higher than the kinetic temperature of the clouds in front of it, the detection of emission lines is direct evidence for inverted populations in high quantum number states of carbon. We also report the detection of C559β line in absorption at 75 MHz with the expected strength.

The detected lines appear at velocities near -47 and -39 km s^{-1}, corresponding to the Perseus arm in this direction. The observed intensity and width of the lines are used to derive the properties of the intervening clouds and to constrain theoretical predictions of level populations in high quantum number states of carbon in cold clouds. In particular, we examine the relevance of the dielectronic effects first discussed by Watson, Western, and Christensen. A comparison of our results with λ-21 cm H I results allows us to identify the source of carbon lines as regions of high density and pressure. The absence of hydrogen recombination lines puts a low upper limit on the hydrogen ionization rate and fractional ionization in these regions. We comment on the thermal balance in these regions.

Subject headings: nebulae: individual (Cas A) — radio sources: lines

I. INTRODUCTION

The importance of stimulated emission of radio frequency recombination lines from ionized regions in the galaxy was first pointed out by Goldberg (1966). Since then, most interpretations of radio recombination lines from H II regions have taken this effect into consideration (e.g., Walmsley 1980). The evidence for this effect is usually indirect, in the form of the departure of line strengths from predictions based on local thermodynamic equilibrium or the correlation of line strength with background nonthermal continuum at low frequencies (Pedlar *et al.* 1978; Anantharamaiah 1985).

One possible direct demonstration of this effect is to detect a recombination line in *emission* from an ionized region lying in front of a strong background source whose brightness temperature is much higher than the kinetic temperature of the ionized region. Such an experiment cannot be done at high frequencies toward an H II region since the brightness temperature of any background source is unlikely to be higher than the typical temperature of an H II region: 8000–10,000 K. At low frequencies (<100 MHz), where this condition is likely to be satisfied, the hydrogen recombination lines from an H II region become undetectable due to pressure broadening or optical depth effects, or both (Shaver 1975).

An excellent direction for observing this effect has been discovered by Konovalenko and Sodin (1980) who detected a line in *absorption* at 26 MHz in the direction of the strong radio source Cassiopeia A. This line, which was attributed by them to a hyperfine transition of interstellar nitrogen, was later correctly identified by Blake, Crutcher, and Watson (1980) as the 631α recombination line of carbon arising in cold clouds along the line of sight. This was subsequently confirmed by Konovalenko and Sodin (1981), who observed the adjacent transition, C630α, also in absorption, with similar optical depth. These lines have now been observed over a wide range of frequencies: 16–30 MHz by Konovalenko (1984), 42–84 MHz by Ershov *et al.* (1984), 26–68 MHz by Anantharamaiah, Erickson, and Radhakrishnan (1985), and 39–118 MHz by Ershov *et al.* (1987).

The principal quantum numbers corresponding to the transitions observed so far are in the range $n = 730$ to $n = 430$. At these low frequencies all the observed lines are in absorption. From simple physical considerations it is easy to see that the recombination lines are expected to be in absorption in this frequency range (Blake, Crutcher, and Watson 1980, Anantharamaiah, Erickson, and Radhakrishnan 1985). At very large n the relative populations of the atomic levels, after recombination, are controlled primarily by collisional processes. This tends to thermalize the population, making the excitation temperature of these levels very close to the kinetic temperature of the gas. We will show that the observed recombination lines of carbon arise in neutral H I clouds which have temperatures of less than 100 K. Toward the strong background source Cas A (brightness temperature $\sim 7.7 \times 10^7$ K at 60 MHz), we therefore expect the recombination lines from these highly excited states to be in absorption.

[1] On leave from Raman Research Institute, Bangalore-560080, India.

At lower n (and correspondingly higher frequencies), however, the relative populations are dominated by radiative processes. This moves the excitation temperature away from the kinetic temperature toward negative values; the level populations become inverted since downward transitions out of a given level are more rapid than the transitions into it from higher levels. This results in stimulated emission of the type discussed by Goldberg (1966). Therefore, at higher frequencies the recombination lines toward Cas A must appear in *emission*, even if the brightness temperature of Cas A is very much higher than the kinetic temperature of the clouds in front of it. This phenomenon must occur regardless of the details of the populating mechanism, although the actual turnover frequency and the strength of the emission lines will depend on these details and also on the density and temperature of the clouds. The dependence of the line parameters on the observing frequency allows these lines to be used as a diagnostics of the physical conditions in the emitting regions.

Shaver (1975) was the first to consider the details of the balance between collisional and radiative effects on the level populations of hydrogen at very large n. He found that stimulated emission should greatly enhance the strength of hydrogen recombination lines from cold clouds in the interstellar medium, especially in the range 50–200 MHz, but that absorption was unlikely except at "very low frequencies," presumably below a few tens of MHz. Further investigations, such as that of Salem and Brocklehurst (1979), revealed that hydrogen recombination lines could be in absorption if the temperature were low enough and the electron density were high enough—conditions not typical for H I clouds.

While investigating the level populations of carbon atoms at very large n, Watson, Western, and Christensen (1980) considered a process similar to dielectronic recombination in addition to the collisional and radiative effects. This process differs from dielectronic recombination in that the atom has insufficient time to emit a photon and become stable. Instead, a lifetime-lengthening process involving collisions with outer electrons provides temporary stability. They found that this process had a profound effect on the level populations in singly ionized carbon, where the ground state has a fine-structure splitting of only 92 K, and predicted that carbon lines could be detected in absorption at frequencies between 250 and 400 MHz. Improved calculations by Walmsley and Watson (1982*b*) showed that under plausible conditions in interstellar H I clouds, carbon recombination lines would be in absorption below 100 MHz, although hydrogen lines would be in emission. Shaver (1976) also considered dielectronic effects available to species other than hydrogen, but only in the case of the intercloud medium with a temperature of $\sim 10{,}000$ K.

In this paper we present observations demonstrating the phenomenon of turnover from absorption to emission in the direction of Cas A. Recombination lines of carbon were observed in this direction at 10 frequencies covering the range 34–325 MHz. The lines appear in absorption below 115 MHz ($n > 385$) and in emission above 200 MHz ($n < 310$). The turnover occurs near 150 MHz ($n \sim 350$). A β-line ($\Delta n = 2$ transition) was also observed in absorption at 75 MHz. Using the observed width and intensity of the lines we derive the density of the intervening clouds and impose constraints on theoretical predictions of level populations in high quantum number states (e.g., Walmsley and Watson 1982*b*). We also observed at frequencies of hydrogen recombination lines between 75 MHz and 325 MHz. No hydrogen line was detected, and the limits are used to derive the ionization and heating rates in these H I clouds.

II. OBSERVATIONS

The observations were made with the 93 m and the 43 m telescopes of the National Radio Astronomy Observatory at Green Bank. The 93 m telescope was used to observe at 34, 52, 70, 78, and 140 MHz. To cover these frequencies we used three different feeds mounted on the traveling feed system: a 20–50 MHz broad-band dipole, a 50–80 MHz tunable crossed dipole, and a 110–250 MHz broad-band crossed dipole. The 384 channel autocorrelator was split into four independent spectrometers of 96 channels each. Total bandwidths of 39 or 78 kHz were used, depending on the frequency of observation. The frequency resolution was 0.41 kHz at 34 MHz, 0.81 kHz at 52, 70, and 78 MHz, and 1.63 kHz at 140 MHz.

The 43 m telescope was used to observe near 75, 115, 220, 240, and 325 MHz. Three broad-band crossed dipole feeds covering 50–88 MHz, 110–250 MHz, and 250–350 MHz mounted at the prime focus were used for the observations. The 1024 channel autocorrelator was split into four independent spectrometers of 256 channels each. The total bandwidths were 78, 156, and 312 kHz. The frequency resolutions were 0.61 kHz at 75 MHz, 1.22 kHz at 115 and 325 MHz, and 2.44 kHz at 220 and 240 MHz.

Near each of the frequencies indicated in Table 1, two or three nearby transitions were observed simultaneously in bands carefully chosen to be interference-free. These spectra were averaged to obtain the final spectrum. Because of the way the different transitions are averaged the velocity scales of the spectra may be in error by up to one spectrometer channel. At 325 MHz the reference spectra were obtained by frequency switching. At all other frequencies reference spectra were measured by switching to a noise source adjusted to balance the total on-source system temperature. In all of the observations the system temperature was dominated by Cas A.

III. RESULTS

Recombination lines of carbon were detected toward Cas A at all the observed frequencies except near 140 MHz. The observed spectra are shown in Figure 1 along with an H I absorption spectrum in the same direction taken from Mebold and Hills (1975).

There are two striking aspects to the spectra shown in Figure 1. First, the observed lines are in absorption below 115 MHz and appear in emission above 220 MHz, as anticipated. Second, the recombination line spectrum near -39 km s^{-1} and -47 km s^{-1} mimics the H I absorption spectrum. These two components correspond to the velocity of the Perseus arm in the direction of Cas A. The presence of two components in the recombination line had not been recognized in previous observations due to insufficient frequency resolution (Konovalenko and Sodin 1980, 1981; Konovalenko 1984; Ershov *et al.* 1984, 1987; Anantharamaiah, Erickson, and Radhakrishnan 1985). The 0 km s^{-1} feature corresponding to the Orion arm is present at the 4 σ level at 325 MHz.

Table 1 gives the parameters of the lines obtained by fitting two Gaussian components (three at 325 MHz) to the observed spectra. As the line-to-continuum ratios are small, the observed optical depths were obtained as $\tau_L = -T_L/T_{\text{Cas A}}$, where T_L is the antenna temperature in the line and $T_{\text{Cas A}}$ is the antenna temperature due to Cas A. During the observations

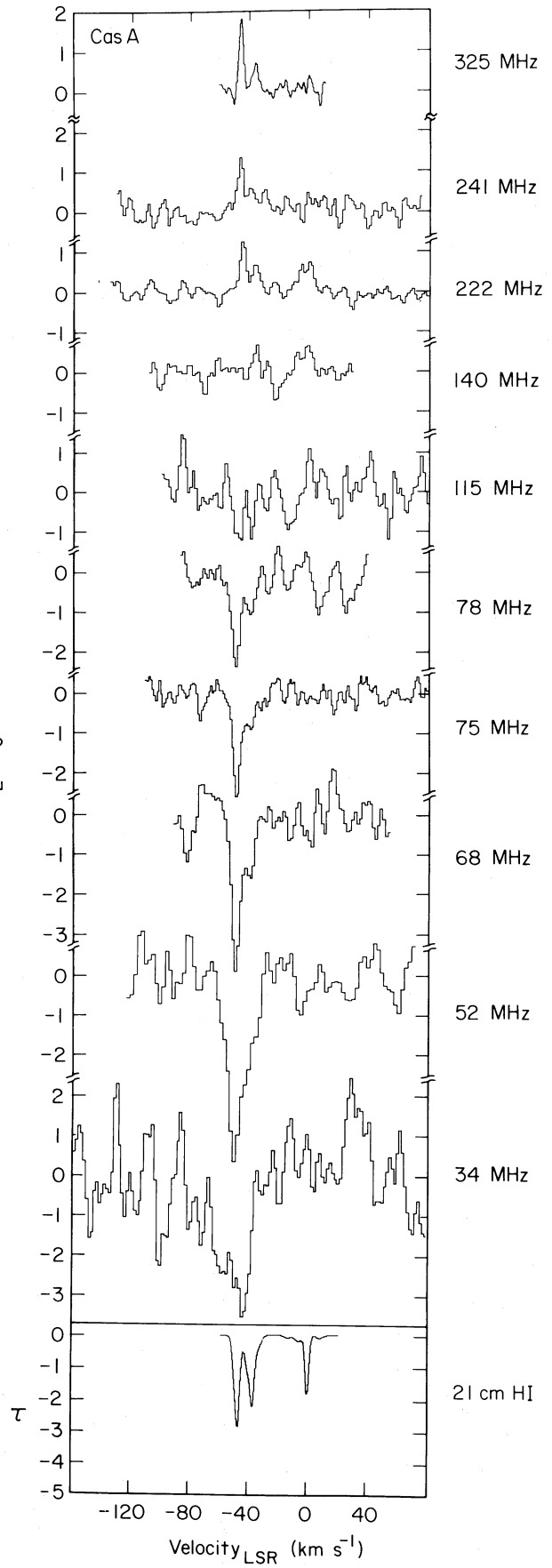

the spectra were normally measured in units of (T_L/T_{sys}), where T_{sys} is the total system temperature when the antenna was pointed toward Cas A. This was corrected by the factor $(T_{sys}/T_{Cas\ A})$ to obtain the optical depth as shown above. The measured value of $(T_{sys}/T_{Cas\ A})$ is given in Table 1.

In these observations we also searched for carbon β lines ($\Delta n = 2$ transition) near 75 and 110 MHz and for hydrogen α lines at 75, 115, 220, and 325 MHz. The carbon β line was detected in absorption at 75 MHz and is shown in Figure 2. For this transition $n = 559$ (C559β). This transition also shows two components at -47 km s^{-1} and -39 km s^{-1}. The parameters of the two components obtained from Gaussian fits are included in Table 1. The α-transition with $n = 559$ occurs near 38 MHz, close to the transitions observed by Anantharamaiah, Erickson, and Radhakrishnan (1985). The ratio of the observed intensities of the α and β lines is ~ 7, which is simply the ratio of the oscillator strengths of the two transitions (Menzel 1968). No hydrogen lines were detected, and the upper limits to the optical depth are indicated in Table 1.

IV. DISCUSSION

a) *Stimulated Emission*

The most interesting result of these observations is that the recombination lines of carbon toward Cas A, which are in absorption below 115 MHz, turn into emission above 200 MHz. The occurrence of an emission line at these frequencies in this direction is direct evidence for stimulated emission of recombination lines. Note that the average brightness temperature of Cas A at 220 MHz is $\sim 4.7 \times 10^6$ K. The emission line indicates that the optical depth in the line is negative and that the corresponding quantum levels have an inverted population.

b) *Pressure and Radiation Broadening*

Another measurable phenomenon at low frequencies is the pressure or radiation broadening of recombination lines. As was discussed by Konovalenko (1984) and Anantharamaiah, Erickson, and Radhakrishnan (1985), the widths of the lines toward Cas A increase dramatically at lower frequencies. These discussions must be modified to account for the presence of two velocity components, separated by 8 km s^{-1}. The Doppler contribution to the line width of each feature is somewhat smaller than assumed by Anantharamaiah, Erickson, and Radhakrishnan (1985), and less than half that deduced by Konovalenko (1984) from data with coarser velocity resolution. Figure 3 is a plot of the measured width of the two components as a function of the principal quantum number. The last point in the plot corresponds to the width of the C559β line. These data indicate that the line broadening is not significant, for either components, over the frequency range observed here. Even so, these measured widths imply upper limits to the electron densities of ~ 0.06 cm^{-3} if the electron temperature is 100 K, and ~ 0.3 cm^{-3} if the temperature is 20 K. Theoretical curves for the expected width of the lines (see below) for two combinations of electron density and temperature are also shown in Figure 3. A slight increase is seen in the width of the C559β line, consistent with the theoretical

FIG. 1.—Carbon α recombination lines ($\Delta n = 1$ transition) observed toward Cas A at 10 frequencies in the range 34–325 MHz. The quantum numbers corresponding to these frequencies are $n = 565$, 502, 450, 440, 435, 385, 360, 310, 300, and 272. The H I absorption spectrum is taken from Mebold and Hills (1975).

TABLE 1

PARAMETERS OF THE OBSERVED LINES[a]

Frequency (MHz)	Transitions Averaged	T_{sys}/T_{cas}	Velocity Resolution (km s^{-1})	V_{lsr} (km s^{-1})	τ_L ($\times 10^3$)	ΔV (km s^{-1})	$\int \tau dv$ (s^{-1})
34	C564α, C565α, C576α	1.41	3.5	−55 ± 4.8	2.26 ± 0.4	27 ± 7	...
				−42 ± 3.3	2.7 ± 1.0	8 ± 3	...
52	C502α, C503α	1.46	4.7	−51 ± 3.3	3.7 ± 0.6	7 ± 1.5	4.7 ± 1.3
				−42 ± 3.3	3.2 ± 0.4	11 ± 2	6.5 ± 1.4
70	C450α, C451α, C456α	1.40	3.4	−50 ± 2.2	3.2 ± 0.4	7 ± 1	5.7 ± 1.1
				−40 ± 2.7	1.7 ± 0.3	7.5 ± 1.5	3.2 ± 0.9
75	C443α, C441α, C445α, C447α	1.69	2.4	−48.1 ± 1.4	2.5 ± 0.1	6.7 ± 0.4	4.3 ± 0.3
			...	−38.9 ± 1.7	0.9 ± 0.1	5.9 ± 1.1	1.6 ± 0.3
	C559β	...	...	−51.2 ± 1.5	0.51 ± 0.07	9.7 ± 1.5	1.32 ± 0.3
				−38.0 ± 1.5	0.53 ± 0.07	9.0 ± 1.4	1.27 ± 0.3
75	H443α, H445α, H447α	...	...		<0.8[b]		
78	C435α, 436α, C437α, C438α	1.26	3.1	−50 ± 2.0	2.3 ± 03	7.5 ± 1	4.8 ± 0.9
				−39.5 ± 2.5	1.0 ± 0.25	6.2 ± 2	1.75 ± 0.7
110	C486β, C487β	1.12	2.2		<1.4[b]		
115	C384α, C385α	1.81	3.2	−48.5 ± 2.6	1.2 ± 0.5	7.3 ± 2	3.5 ± 1.7
				−40 ± 2.6	1.2 ± 0.5	3.5 ± 1.7	1.7 ± 1.1
115	H384α	...	...		<1.4[b]		
140	C358α, C359α	1.17	3.4		<0.7[b]		
	C360α, C362α	...	...				
220	C308α, C310α	1.69	3.3	−45.6 ± 2.0	−1.0 ± 0.1	7.6 ± 1.0	−6.0 ± 1.0
				−36.3 ± 2.2	−0.6 ± 0.1	5.7 ± 1.3	−2.9 ± 0.8
220	H308α	...	...		<0.5[b]		
240	C300α, C301α	1.69	3.0	−48.2 ± 1.8	−1.3 ± 0.15	5.0 ± 0.7	−5.5 ± 1.0
	C302α, C303α	...	...	−40.5 ± 2.2	−0.6 ± 0.15	5.6 ± 1.8	−2.7 ± 1.1
325	C272α, C273α	1.12	1.2	−47.1 ± 0.7	−1.83 ± 0.08	3.22 ± 0.16	−6.8 ± 0.4
				−37.7 ± 0.8	−0.63 ± 0.05	4.8 ± 0.5	−3.5 ± 0.5
				−0.7 ± 0.9	−0.39 ± 0.1	2.2 ± 0.6	−1.0 ± 0.5
325	H272α, H273α	...	...		<1.5[b]		

[a] Errors quoted are 1 σ values.
[b] 3 σ upper limits.

curves. The β-lines may be particularly useful for future measurements of pressure broadening. The α-lines are broadened significantly below 30 MHz (Konovalenko 1984), but it is exceedingly difficult to observe at these frequencies because of terrestrial interference. The corresponding β-lines occur at frequencies twice as high.

To extend the comparison to lower frequencies we reinterpret the data of Konovalenko (1984) and Ershov *et al.* (1984, 1987), assuming their line widths are too wide by ~8 km s^{-1}, the separation between the two features, since the depths of the two features appear to be similar at the lowest frequencies. We have calculated the expected line broadening according to formulae in Shaver (1975). Pressure broadening is calculated from a low-temperature approximation:

$$\Delta v_P = 2 \times 10^{-8} T_e^{-3/2} e^{-26/T_e^{1/3}} n_e n^{5.2} \text{ kHz} , \quad (1)$$

where T_e is the electron temperature and n_e is the electron density. Radiation broadening is calculated from

$$\Delta v_R = 8 \times 10^{-20} W_\nu T_R n^{5.8} \text{ kHz} , \quad (2)$$

where T_R is the equivalent blackbody temperature of the background nonthermal radiation field, measured at 100 MHz, and W_ν is the dilution factor. A spectral index of −2.6 has been assumed. We used $T_R = 800$ K and $W_\nu = 1$, the values used by Walmsley and Watson (1982*b*). If all of these broadening effects are present, then the resulting line profile is a Voigt profile, i.e., the convolution of a Gaussian profile with a Lorentzian profile. Following Konovalenko (1984) we estimate the half-power line width to be approximately

$$\Delta v_L = [(\Delta v_P + \Delta v_R)^2 + \Delta v_D^2]^{1/2} , \quad (3)$$

where Δv_D is the Doppler contribution to the line width. Shaver (1975) estimates the accuracy of such an approximation to be at worst ~20% in the region where the Gaussian and Lorentzian component widths are comparable.

Doppler widths of 6.7 km s^{-1} for the −47 km s^{-1} feature and 5.9 km s^{-1} for the −39 km s^{-1} features were chosen to reproduce the observed widths at 75 MHz. For electron temperatures of 100 K, 50 K, and 20 K the electron density was varied to obtain a reasonable fit to the 25–30 MHz data from Konovalenko (1984). Since we assumed that both features have the same width at these low frequencies, essentially the same electron densities were found for both the features. Acceptable combinations of electron temperature and density are 100 K and 0.055 cm^{-3}, 50 K and 0.08 cm^{-3}, and 20 K and 0.27 cm^{-3}. Data for the −47 km s^{-1} feature are shown in Figure 4. Three of the data points from Ershov *et al.* (1984, 1987) do not fit the theoretical curves. Our assumed galactic nonthermal radiation field is slightly weaker than that used by Konovalenko (1984) or Ershov *et al.* (1984). Using their field would result in electron densities ~20% smaller.

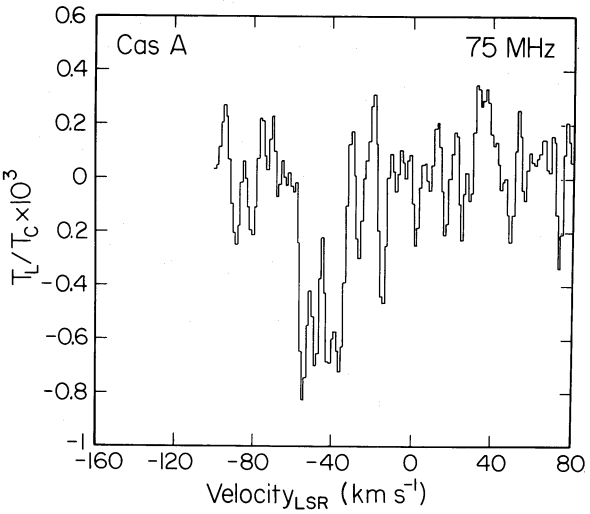

FIG. 2.—C559β line ($\Delta n = 2$ transition) observed at 75 MHz toward Cas A

c) *Strength of the Observed Lines—Comparison with Predictions*

Although the phenomenon of turnover from absorption to emission is expected from simple physical arguments, the actual frequency of turnover and the strength of the lines will depend on the physical conditions in the cloud. It will also depend on the populating mechanism for the carbon atoms. The dielectronic effects discussed by Watson, Western, and Christensen (1980) will be important if the temperature is in the range 50–100 K. We will first discuss this possibility and then discuss the low-temperature models favored by Ershov *et al.* (1984, 1987).

i) *High-Temperature ($T_e > 50$ K) Models with Dielectronic Effects*

For electron densities less than 0.1 cm^{-3} (as implied by the line widths at low frequencies, if $T_e > 50$ K) pure hydrogenic population of the high quantum number states predicts that the lines will be in emission up to $n = 600$ or higher (Walmsley and Watson 1982*b*). In order to account for absorption lines at 26 MHz ($n = 632$), Walmsley and Watson (1982*a*, *b*) have invoked a dielectronic recombination-like process which has considerable influence on the population of very high n states. This process, first described by Watson, Western, and Christensen (1980), involves the capture of an electron with positive energy with the simultaneous excitation of the ground-state fine-structure transition ($^2P_{1/2} \rightarrow {}^2P_{3/2}$). The process requires incident electrons with thermal energies near the energy splitting of the ground-state, 92 K, and so should operate efficiently at the temperatures typical of H I λ-21 cm absorbing clouds (Payne, Salpeter, and Terzian 1983) but become ineffective at very low temperatures.

Incorporating this process, Walmsley and Watson (1982*b*) have computed the departure coefficients b_n and β_n for different electron densities and temperatures, where b_n is the ratio of the population of level n to its thermodynamic equilibrium population, and β_n is related to the derivative of b_n with respect to n. Our data indicate that the turnover from absorption to emission occurs somewhere between $n = 310$ and $n = 380$, probably near $n = 350$ or 155 MHz. The grid of models provided by Walmsley and Watson (1982*b*) is sparse, but the model with $n_e = 0.1$ cm^{-3} and $T_e = 100$ K and a subthermal ratio of fine-structure level populations has its turnover within this range. For $T_e = 50$ K, the turnover is close to $n = 400$. At this density, hydrogenic, and thermal fine-structure population models all have turnovers below 35 MHz ($n > 550$). The fine-structure level populations will be controlled by the galactic nonthermal radiation and collisions with neutral atoms and molecules and should not depend on the degree to which carbon is depleted (Watson, Western, and Christensen 1980). Increasing the strength of the galactic nonthermal radiation would move the crossover between absorption and emission to lower n, and might make the $T_e = 50$ K model more viable. On the other hand, the electron density of the $T_e = 100$ K model is about a factor of 2 higher than appropriate; decreasing the electron density appears to move the crossover to higher n.

Figure 5 is a plot of the observed integrated optical depth for the two components. The optical depth in the center of an α-recombination line is given by (Salem and Brocklehurst 1979)

$$\tau_{Cn} = \frac{5.76 \times 10^5}{\nu T_e^{5/2} \Delta V} \left(\frac{n_{C^+}}{n_e}\right) \mathrm{EM_C} \beta_n b_n \qquad (4)$$

where ν is the line frequency (MHz), ΔV is the full width at half-maximum of the line (km s^{-1}), n_{C^+} is the density of singly ionized carbon ions, and $\mathrm{EM_C} = n_e^2 l$ is the emission measure (cm^{-6} pc) in the carbon line region, where l is the path length through the cloud [pc].

Using equation (4) and the calculations of b_n and β_n by Walmsley and Watson (1982*b*) we can compute the expected variation of the integrated optical depth ($\propto \tau \Delta v$) as a function of the principal quantum number n. We have plotted this curve in Figure 5 for $n_e = 0.1$ cm^{-3} and $T_e = 100$ K (*heavy solid line*)

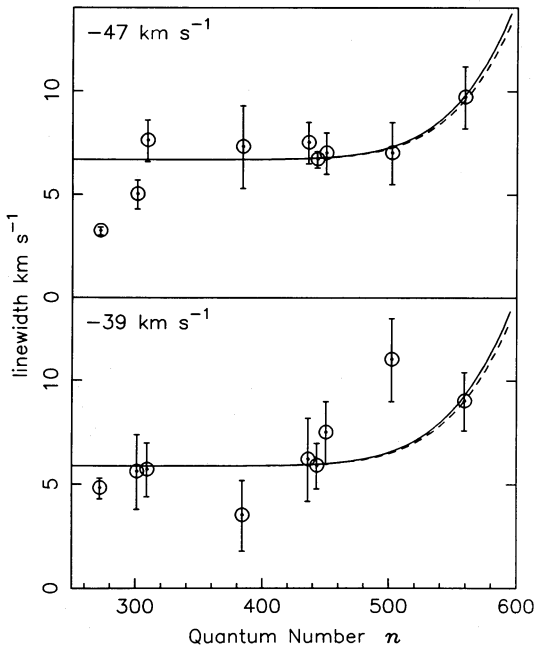

FIG. 3.—Observed width of the recombination lines as a function of the principal quantum number. The top and bottom panels correspond to the two velocities of the Perseus arm. The solid and the dashed lines are the expected width based on a combination of pressure and radiation broadening. The expected width is calculated using the formula in Shaver (1975) and assuming a temperature and electron density of 100 K and 0.06 cm^{-3}, respectively, for the solid curve and 20 K and 0.3 cm^{-3} for the dashed curve. Doppler widths of 6.7 km s^{-1} and 5.9 km s^{-1} were used for the top and bottom curves, respectively.

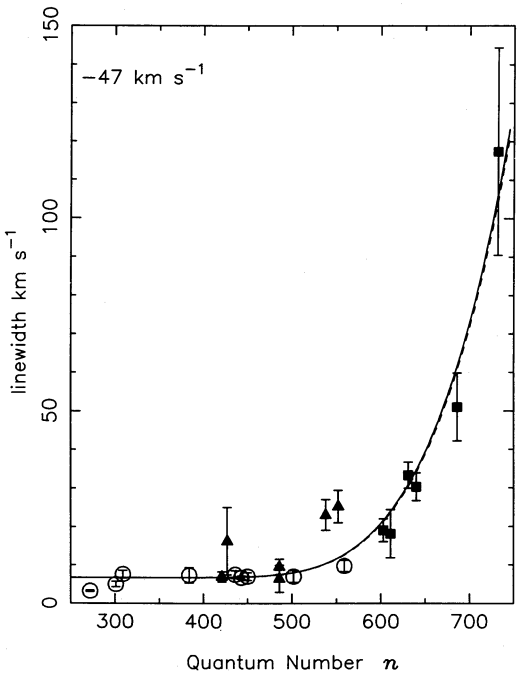

FIG. 4.—Width of the lines for the entire quantum number range observed toward Cas A. The open circles are from the present observations. The filled triangles are from Ershov *et al.* (1984) and Ershov *et al.* (1987). The filled squares are from Konovalenko (1984). The observed values from Ershov *et al.* and Konovalenko have been reduced by 8 km s^{-1} to account for the presence of two components at −47 km s^{-1} and −39 km s^{-1}. The solid and the dashed curves are theoretical predictions based on a combination of radiation and pressure broadening (*see text*). The solid curve corresponds to an electron temperature of 100 K and an electron density of 0.055 cm^{-3}. The corresponding values for the dashed curves are 20 K and 0.27 cm^{-3}, respectively. A radiation temperature of 800 K at 100 MHz with a spectral index of −2.6 was assumed for computing the radiation broadening.

and 50 K (*thin solid line*). We assumed that all the electrons came from singly ionized carbon ($n_{C^+}/n_e = 1$). The curves are normalized to match the observed value near $n = 450$. The normalization fixes the value of $n_e n_{C^+} l$ for the −47 km s^{-1} and −39 km s^{-1} features, respectively, to 0.0062 cm^{-6} pc and 0.0022 cm^{-6} pc if $T_e = 100$ K, and to 0.0068 cm^{-6} pc and 0.0025 cm^{-6} pc if $T_e = 50$ K. Clearly, the model with $T_e = 50$ K does not fit the observations—the crossover is in the wrong place. For the −39 km s^{-1} feature, the model with $T_e = 100$ K and $n_e = 0.1$ cm^{-3} gives a reasonable fit both to the turnover frequency and the observed variation of line strength in the range $270 < n < 500$, but the predicted strength of the emission lines is less than observed. This model does not fit the observed variation of the line strength for the −47 km s^{-1} feature, although the turnover frequency is predicted correctly. A comparison of the models of Walmsley and Watson (1982*b*) indicates that reducing the electron density would lead to relatively stronger emission lines, so a model with the appropriate electron density for this temperature would give a better fit to the data.

In Figure 6 we have plotted the integrated optical depth for the entire range of observed quantum numbers ($n = 272$ to $n = 732$). The lower frequency data are taken from Konovalenko (1984) and Ershov *et al.* (1984). For the purpose of this plot we have added the contribution to the integrated optical depth from both of the components given in Table 1. This is necessary since the observations of Konovalenko (1984) and Ershov *et al.* (1984) did not resolve the two components. The theoretical curves are the same as those shown in Figure 5. In addition to the failure to predict the strength of the emission lines, there is a problem at the lowest frequencies. The models predict a strong increase in the integrated optical depth as n increases, but the data show relatively little increase. The discrepancy for the absorption lines could be mitigated if the results of Konovalenko (1984) were scaled up by about a factor of 2 with respect to our data. Perhaps these two sets of data are miscalibrated with respect to each other because we overestimated ($T_{sys}/T_{Cas\ A}$) or he underestimated it.

In summary, the available models from Walmsley and Watson (1982*b*) do not provide a satisfactory fit to the dependence of the integrated optical depth on principal quantum number n. On the other hand, an examination of the models indicates that the modifications in the model parameters required to match the deduced electron density would improve the fit to the data. An increase in the assumed value of the galactic nonthermal background might even allow a satisfactory fit for $T_e = 50$ K. The discrepancy at the lowest frequencies is serious, unless it is due to differences in calibration.

ii) *Low-Temperature ($T_e < 20$ K) Models*

Ershov *et al.* (1984), analyzing the observations then available, concluded that the variation of line strength with fre-

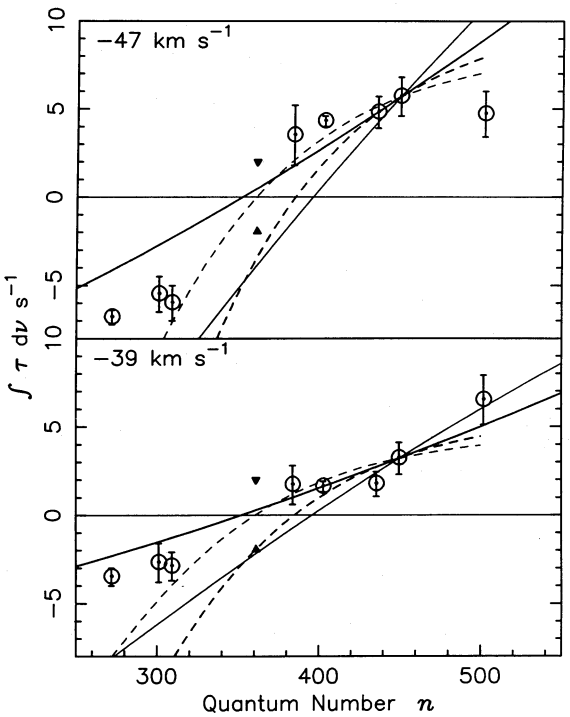

FIG. 5.—Observed integrated line strength for the two components corresponding to the velocities of the Perseus arm. The filled triangles near $n = 360$ represent upper limits to emission and absorption. The solid lines are predicted variation of line strength for high-temperature models (*see text*), which include dielectronic effects (Walmsley and Watson 1982*a*). For the thick solid line the combination of temperature and electron density are 100 K and 0.1 cm^{-3}, respectively, and for the thin solid line the values are 50 K and 0.1 cm^{-3}. The dashed lines are predicted variation for low-temperature models where the level populations are purely hydrogenic (Salem and Brocklehurst 1979). The temperature and electron density for the thick dotted line are 20 K and 0.27 cm^{-3}, respectively, and for the thin dotted line the values are 16 K and 0.4 cm^{-3}. In all the cases, the predictions are normalized to match the observed value near $n = 450$.

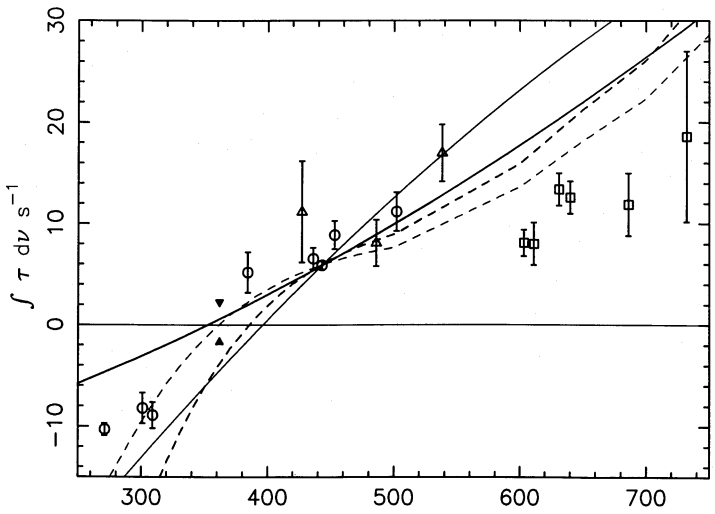

FIG. 6.—Sum of the integrated line strength of the two components at −47 and −39 km s^{-1} for the entire quantum number range observed toward Cas A. The open circles are from the present observations. The triangles are from Ershov *et al.* (1984) and Ershov *et al.* (1987). The squares are from Konovalenko (1984). The filled triangles near $n = 360$ represent upper limits to emission and absorption. The solid lines are predicted variation of line strength for high-temperature models (*see text*), which include dielectronic effects (Walmsley and Watson 1982*a*). For the thick solid line the combination of temperature and electron density are 100 K and 0.1 cm^{-3}, respectively, and for the thin solid line the values are 50 K and 0.1 cm^{-3}. The dashed lines are predicted variation for low-temperature models where the level populations are purely hydrogenic (Salem and Brocklehurst 1979). The temperature and electron density for the thick dotted line are 20 K and 0.27 cm^{-3}, respectively, and for the thin dotted line the values are 16 K and 0.4 cm^{-3}. For the low-temperature models, the predictions for $n > 500$ are extrapolations based on calculations by Walmsley and Watson (1982*b*) for a temperature of 20 K and electron density of 1.0 cm^{-3}. In all the cases, the predictions are normalized to match the observed value near $n = 450$.

quency may be fitted by models with a temperature below 20 K and either (1) hydrogenic level populations or (2) level populations that include dielectronic effects in the case where the carbon fine-structure level populations have their thermodynamic equilibrium values. At a temperature of 20 K, the dielectronic effects are small. The electron density in the low-temperature models is ~0.3 cm^{-3}, requiring a total density near 10^3 cm^{-3} if all the electrons came from carbon. Ershov *et al.* (1984) argue that if carbon were depleted from the gas phase by a factor of 5 or more, then the total density would be high enough to make the carbon fine-structure level populations approach their thermal equilibrium values. And if the cooling from the carbon fine-structure lines were balanced against the heating from carbon photoionization alone, then the thermal equilibrium temperature would be below 20 K, independent of the density or the degree to which carbon is depleted. These models give a better fit to data between 16 MHz and 84 MHz than selected models with higher temperatures and dielectronic effects with subthermal excitation of the fine-structure levels, i.e., models similar to those discussed above. However, the electron densities selected for these higher temperature models are considerably higher than the ones we used.

We have obtained hydrogenic departure coefficients by interpolating between the results of Salem and Brocklehurst (1979)—however, results for temperatures below 25 K are actually an extrapolation. In Figures 5 and 6, we have plotted the variation of line strength predicted by low-temperature models with hydrogenic populations. The thick dotted line is for $T_e = 20$ K and $n_e = 0.3$ cm^{-3}, and the thin dotted line is for $T_e = 16$ K and $n_e = 0.4$ cm^{-3}. These models are again normalized to the data at $n = 445$, yielding values of $n_e n_{C^+} l$ for the −47 km s^{-1} and −37 km s^{-1} features, respectively, of 0.0024 cm^{-6} pc and 0.00086 cm^{-6} pc if $T_e = 16$ K, and 0.0058 cm^{-6} pc and 0.0021 cm^{-6} pc if $T_e = 20$ K. The model with $T_e = 20$ K is similar to the one discussed by Ershov *et al.* (1984) and predicts crossovers between absorption and emission somewhere between $n = 380$ and $n = 400$, which is slightly too high. This model predicts emission at $n = 360$, which we should have seen at more than the 5 σ level. The model with a temperature of 16 K and an electron density of 0.4 cm^{-3} satisfies both the line broadening and crossover frequency constraints. The fit to the high-frequency, emission-line data is remarkably good, except for the highest frequency point. The line strength at $n = 272$ is overestimated by more than a factor of 2, which is 10 σ away from the measured value. The hydrogenic departure coefficients for principal quantum numbers $n > 500$ are also an extrapolation, based on a calculation by Walmsley and Watson (1982*a*) for a temperature of 20 K and an electron density of 1 cm^{-3}, somewhat higher than the density over the rest of the curve. The dotted curves in Figure 6 rise considerably above the observed points from Konovalenko (1984), which again may be due to differences in calibration or to problems with the extrapolation.

The models that include dielectronic effects but assume the carbon fine-structure levels to be populated according to thermodynamic equilibrium may not be relevant. Even if the electron density were as high as 0.4 cm^{-3} and came entirely from a cosmic abundance of carbon, the required total density is ~1000 cm^{-3}. At this density, the upper fine-structure state would still be underpopulated by a factor of ~4, compared to its thermodynamic equilibrium population (Watson, Western, and Christensen 1980). The large gas phase depletions mentioned by Ershov *et al.* (1984) are no longer considered common, although they are seen in some parts of the sky (Jenkins and Shaya 1979). It therefore seems unlikely that the density could be high enough to thermalize the fine-structure level populations.

In conclusion, both the high-temperature models with dielectronic effects and the low-temperature models with hydrogenic populations only marginally fit the observed variation of the line strength. All of these models overestimate the strength of the lines with $n > 600$, but this may indicate a problem with the relative calibration of the data. The models also have prob-

lems at low n. The hydrogenic models may be suffering from the extrapolation from higher temperatures, while the dielectronic models suffer from the lack of computations with appropriate combinations of electron temperature and density.

d) Electron and Neutral Density of the Clouds

The spectra shown in Figure 1 demonstrate the similarity of the profile shapes of the carbon recombination lines and the neutral hydrogen absorption lines in the Perseus arm. This may suggest a common origin for the two lines. (On the other hand, OH and H_2CO absorption lines span the same velocities, and the -47 km s^{-1} and -39 km s^{-1} features are present, but they do not dominate these spectra to the degree that they dominate the H I spectrum.) In this section, we examine the possibility of explaining both the neutral hydrogen and carbon recombination line results, assuming that the lines originate in the same gas. We will discuss the two models introduced in the previous section: (1) a model based on the departure coefficients calculated by Walmsley and Watson (1982*b*) for a temperature of 100 K and electron density of 0.1 cm^{-3}, including dielectronic effects and a subthermal population of ionized carbon fine-structure levels and (2) a lower temperature model with $T_e = 16$ K, $n_e = 0.4$ cm^{-3} and hydrogenic level population calculations from Salem and Brocklehurst (1979). For model (1), the electron density of 0.1 cm^{-3} is too high to be consistent with the observed line broadening, and so a value of 0.055 cm^{-3} is used in expressions where the electron density appears explicitly. The galactic nonthermal radiation field is not the same in the two departure coefficient calculations, but for electron densities as high as those of model (2), the departure coefficients should not be very sensitive to variations in the radiation field.

i) *High-Temperature Models*

Neutral hydrogen spin temperature measurements toward Cas A seem to rule out a temperature as high as 100 K. Mebold and Hills (1975) performed λ-21 cm H I emission-absorption observations toward Cas A, and derived neutral hydrogen spin temperatures for the -47, -39, and 0 km s^{-1} features of 77 K, 88 K, and 100 K, respectively. These temperatures are upper limits to the physical temperature in the absorbing clouds because the spin temperature is an average temperature along the line of sight, and although it is weighted in favor of the coldest regions, warm intercloud gas will also make a contribution. For example, Payne, Salpeter, and Terzian (1983) modeled a wide range of observed spin temperatures as due to absorbing clouds at $\sim$55 K but with different column densities, all surrounded by identical warm envelopes.

Spin temperature determinations rely on comparison fields to determine the emission. If the fraction of the solid angle of Cas A covered by the absorbing cloud (the covering factor) is different from the covering factor in the comparison fields (usually called the beam filling factor), then the spin temperature can be biased upward or downward, depending on whether the Cas A covering factor is less than or greater than average. The uncertainty is worst for galactic plane sources like Cas A, where distant clouds give rise to structure on small angular scales. Therefore, the measured spin temperatures toward Cas A probably indicate physical temperatures below $\sim$75 K for neutral hydrogen in the Perseus arm, but higher temperatures cannot be ruled out. For this reason, these calculations should be regarded as illustrative, rather than definitive.

From equation (4) the ratio of the optical depths of carbon and hydrogen recombination lines from the same cloud at a given frequency is

$$\frac{\tau_{Cn}}{\tau_{Hn}} = \frac{n_{C^+}}{n_p} \frac{[b_n \beta_n]_C}{[b_n \beta_n]_H}, \tag{5}$$

where we have assumed that the widths of the lines are the same. Subscripts C and H represent the departure coefficients for carbon and hydrogen, respectively, and n_p is the proton density in the cloud. Note that this ratio is independent of the covering factor of the background source. Using equation (5) and the lower limit to the ratio of the optical depths at 220 MHz from Table 1 we get a lower limit to the ratio of carbon ions to protons of 3.4 for the -47 km s^{-1} cloud and 2.0 for the -39 km s^{-1} cloud. If all the electrons come from carbon and hydrogen, then this implies a lower limit to the ratio $[n_{C^+}/n_e]$ of 0.77 and 0.67 for the two clouds. Data from the other frequencies where both carbon and hydrogen line frequencies were observed put weaker limits on this ratio.

Emission measures were determined to within a factor of $[n_{C^+}/n_e]$ by the normalization of the models to the data. If the electron density in each cloud is 0.055 cm^{-3}, and $[n_{C^+}/n_e]$ is in the range from 1.0 to the values given above, then the path lengths through the clouds at -47 km s^{-1} and -39 km s^{-1}, respectively, must be in the ranges 2.0–2.7 pc and 0.7–1.1 pc. The column densities of singly ionized carbon, N_{C^+}, are 3.5×10^{17} cm^{-2} for the -47 km s^{-1} feature and 1.3×10^{17} cm^{-2} for the -39 km s^{-1} feature. Note that the total emission measure is a factor of 40 below the upper limit imposed by the low-frequency continuum absorption if the electron temperature were 100 K (Bridle 1969).

From the observed H I optical depths and line widths, and assuming a spin temperature of 100 K, we estimate that the column density of neutral hydrogen N_{HI} is 3.0×10^{21} cm^{-2} and 1.4×10^{21} cm^{-2} in the two clouds. The derived H I column densities depend linearly on the spin temperature.

If the covering factor of Cas A by the clouds is less than one, then both H I and recombination line optical depths will be underestimated, as will the emission measure, path length, and column densities—all by the same factor. A comparison of interferometric H I λ-21 cm data (e.g., Goss, Kalberla, and Dickel 1984) with single-dish data indicates that optical depths could easily be underestimated by a factor of 2. Also, at the distance of the Perseus arm the angular size of Cas A corresponds to a transverse linear size of $\sim$5 pc, which is several times our derived path lengths, suggesting a covering factor less than unity.

Combining the H I column densities with the path lengths derived from the recombination lines implies H I space densities n_{HI} in the range 360–480 cm^{-3} for the -47 km s^{-1} feature, and 410–650 cm^{-3} for the -39 km s^{-1} feature. If all the electrons come from carbon, then the higher densities apply. For both features the derived pressure is high—at least 4×10^4 cm^{-3} K. (Note, however, that if we had assumed the spin temperature to be 50 K, then the densities would be in the range 250–370 cm^{-3} for the -47 km s^{-1} feature, and 220–370 cm^{-3} for the -39 km s^{-1} feature, and the pressures would be lower, although still high.) Because these space densities and pressures ultimately depend on the ratio of H I and recombination line optical depths, they do not depend on the unknown covering factor. The only uncertainties are those of the departure coefficient calculations and the temperature of the clouds.

Other ratios that are reliable in the sense that they do not depend on the covering factor are, the relative abundance of

ionized carbon to neutral hydrogen, $[N_{C^+}/N_H]$, which is $\sim 1.2 \times 10^{-4}$ and 0.9×10^{-4} for the -47 km s^{-1} and -39 km s^{-1} features, respectively, and the ratio $[n_e/n_H]$, which must be between 0.8×10^{-4} and 1.5×10^{-4}. Compared to its cosmic abundance (Spitzer 1978), carbon seems to be depleted by about a factor of 3. Since additional hydrogen could be present in molecular form, this is a lower limit to the depletion factor. A reliable upper limit on the fractional ionization of hydrogen $x = [n_p/n_H]$ is obtained by allowing $[n_{C^+}/n_e]$ to take its minimum value and assuming that the rest of the electrons come from hydrogen; the values obtained are 3.5×10^{-5} for the -47 km s^{-1} feature, and 4.4×10^{-5} for the -39 km s^{-1} feature. (If we had assumed the spin temperature to be 50 K, then we would have found the carbon depletion factor to be ~ 1.5 and the fractional ionization of hydrogen to be less than $\sim 7 \times 10^{-5}$ and 9×10^{-5} in the two features.)

ii) *Low-Temperature Models*

Consider now the model in which the level populations of carbon are hydrogenic. Then, the ratio $[n_{C^+}/n_p]$ is simply the ratio of carbon and hydrogen recombination line optical depths. If all the electrons come from carbon and hydrogen, then the lower limits to $[n_{C^+}/n_e]$ are 0.76 and 0.53 for the features at -47 km s^{-1} and -39 km s^{-1}, respectively. Again taking the value of $[n_{C^+} n_e l]$ from the normalization of the models to the data, and taking into account the allowed variation in $[n_{C^+}/n_e]$, assuming an electron density of 0.4 cm^{-3} implies path lengths of only 0.015–0.020 pc for the -47 km s^{-1} feature and 0.005–0.010 pc for the -39 km s^{-1} feature. The column density of ionized carbon is 1.8×10^{16} cm^{-2} and 0.7×10^{16} cm^{-2} in the -47 km s^{-1} and -39 km s^{-1} features, respectively. Recall that the emission measure, path length, and column density are underestimated if the covering factor of the source is less than unity. The very short path lengths strongly indicate a small covering factor.

Assuming all of the observed H I λ-21 cm optical depth is contributed by gas at 16 K would imply column densities of 0.48×10^{21} cm^{-2} and 0.22×10^{21} cm^{-2} for the features at -47 km s^{-1} and -39 km s^{-1}, respectively. Putting that column density along the short path lengths derived above would result in space densities as high as 10^4 cm^{-3} and pressures p/k greater than 10^5 cm^{-3} K. These values do not depend on the unknown covering factor and are simply the result of assuming that the same gas is responsible for the carbon recombination lines and the H I λ-21 cm lines. Because these values are so high, it appears that only a fraction of the observed H I optical depth can be contributed by gas at 16 K. However, we have no way of determining what that fraction is, and so we cannot derive densities, pressures, or depletion factors.

To return for a moment to the matter of the observed H I spin temperature, there must be a considerable column density of warmer H I to raise the measured spin temperature to above 75 K. If the observed spin temperature is explained by invoking an envelope of hot, nonabsorbing H I, and if the temperature of the cold H I is only 16 K, then the column density of warm H I must be at least 6 times that of the cold H I to make the observed spin temperature be 75 K. If the warm H I also makes a contribution to the optical depth at λ-21 cm, as argued in the previous paragraph, then its temperature cannot be too warm, and the ratio of warm to cold column densities must be even larger. But then, the carbon recombination lines from this warmer gas should be quite conspicuous, and the question arises as to why the observed recombination lines should be attributed to the cold gas.

e) Ionization Rate of Hydrogen

From the absence of hydrogen recombination lines we can derive upper limits to the fractional ionization and ionization rates in the hydrogen clouds at -47, -39, and 0 km s^{-1}. For our higher temperature model, we loosely follow the procedure given by Shaver (1976) and used by Payne, Salpeter, and Terzian (1984), which assumes that the recombination lines and λ-21 cm H I absorption arise in the same gas. For the low-temperature model, we follow the procedure of Sorochenko and Smirnov (1987). As emphasized by Sorochenko and Smirnov (1987), the fact that the carbon recombination lines are actually detected makes these determinations much more robust than in the earlier investigations—we are able to constrain the relationship between electron temperature and density.

In equilibrium, ionization balances recombination and we have $\zeta_H n_{HI} = \alpha^{(2)} n_e n_p$ where ζ_H is the ionization rate, and $\alpha^{(2)}$ is the recombination coefficient to all levels except the ground state. Shaver (1977) pointed out that the optical depth in the λ-21 cm line is proportional to n_{HI} and that the hydrogen recombination line optical depth is proportional to $n_e n_p$. The path length through the cloud drops out when the ratio of the optical depths is taken, as does the covering factor. The remaining factors depend only weakly on T_e and n_e. Based on the derivation of Shaver (1977) we can write

$$\zeta_H = 1.9 \times 10^{-12} \left(\frac{\tau_{Hn}}{\tau_{HI}}\right) \left(\frac{\Phi_2}{3.36}\right) \left(\frac{\nu}{100 \text{ MHz}}\right) \times \left(\frac{T_e}{T_S}\right) \frac{(T_e/100 \text{ K})}{(b_n \beta_n)_H} \text{ s}^{-1} \quad (6)$$

where Φ_2 is an integral over Gaunt factors (Spitzer 1978) which depends weakly on the temperature. Assuming $T_e = T_S = 100$ K and using b_n and β_n from Walmsley and Watson (1982*b*), our upper limit to the optical depth of hydrogen recombination lines (τ_{Hn}) at 220 MHz (Table 1) implies $\zeta_H < 3.9 \times 10^{-17}$ s^{-1}, 5.6×10^{-17} s^{-1}, and 7.6×10^{-17} s^{-1} for the features at -47, -39, and 0 km s^{-1}, respectively. We have used τ_{HI} from Mebold and Hills (1975). There are few uncertainties in these numbers other than those of the departure coefficient calculations. These rates are comparable to those derived by Casse and Shaver (1977) based on their limit to the hydrogen recombination lines at 242 MHz. These upper limits are only slightly above the expected floor to the ionization rate supplied by cosmic rays (Spitzer and Jenkins 1975) and are comparable to the low ionization rate toward ζ Oph (Black and Dalgarno 1977; Crutcher and Watson 1981).

In § IV*d* we combined a carbon recombination line emission measure derived by model fitting with a neutral hydrogen column density derived from the λ-21 cm H I absorption to obtain direct estimates of x, the fractional ionization of hydrogen. From the ratio of hydrogen to carbon recombination line optical depths we set an upper limit on the proton density n_p, and the neutral hydrogen density was determined from the H I column density and a path length derived from the carbon emission measure. Simply inserting these values into the relation $\zeta_H = \alpha^{(2)} n_e x$, yields the even lower ionization rates of 1.3×10^{-17} s^{-1} and 1.7×10^{-17} s^{-1} for the -47 km s^{-1} and -39 km s^{-1} features, respectively. Why are these rates only a third of those derived from equation (6)? For one thing, the model fitting underestimates the strength of the line at 220 MHz by about a factor of 2; correcting for this would imply a longer path length and hence a lower neutral hydrogen space density and a correspondingly higher fractional ionization.

Second, this method uses integrated optical depths rather than peak optical depths, and the recombination lines are wider than the H I absorption lines by about a factor of 1.5.

If the temperature is actually 16 K, then the hydrogen recombination lines are expected to be considerably weaker, so failing to detect them would put weaker limits on the ionization rate. Setting $\Phi_2 = 4.3$ (Spitzer 1978) and using the departure coefficients from Salem and Brocklehurst (1979) the data at 220 MHz imply $\zeta_H < 2.6 \times 10^{-16}$ s^{-1}, 3.4×10^{-16} s^{-1}, and 4.1×10^{-16} s^{-1} for the features at -47, -39, and 0 km s^{-1}, respectively. We have shown that only a fraction of the H I can be at 16 K, but because the H I optical depth and hydrogen recombination line optical depths have a similar dependence on temperature, equation (6) should remain approximately valid as long as the temperature of the rest of the absorbing gas is not too high—say below 50 K.

An alternative approach, presented by Sorochenko and Smirnov (1987), is to use the hydrogen to carbon recombination line optical depth ratio as the ratio of the proton density n_p to the ionized carbon density n_{C^+} and then to assume that the ratio of the carbon ion density to the neutral hydrogen density $n_{H\,I}$ is the cosmic abundance ratio, 3.3×10^{-4}. If we apply this approach to our data at 75 MHz, we obtain fractional ionizations x of 1.1×10^{-4} and 2.9×10^{-4} for the features at -47 km s^{-1} and -39 km s^{-1}, respectively. Inserting these values into the ionization balance equation yields ionization rate upper limits of 1.0×10^{-15} s^{-1} and 2.6×10^{-15} s^{-1} for the two features. Sorochenko and Smirnov (1987) have already shown that the lower frequency data yields the much lower upper limit of 1.5×10^{-16} s^{-1}.

f) Thermal Balance in the Clouds

Given the low fractional ionization and ionization rate we can ask whether it is possible to maintain the observed clouds at a temperature as high as 100 K. Under the conditions derived for model (1) the primary cooling channel is the fine-structure transition in the ground state of ionized carbon atoms, excited by collisions with hydrogen atoms:

$$H + C^+(^2P_{1/2}) \rightarrow H + C^+(^2P_{3/2})$$

The fractional ionization is so low that the collisions between electrons and carbon ions can be ignored. For ionization rates as low as are inferred here, the heating will be dominated by photoelectric emission from grains (Draine 1978). The column density of these clouds is too high to allow soft X-rays to penetrate them and heat the clouds.

Draine (1978) has modeled the steady state temperatures of diffuse clouds in the presence of photoelectric heating by grains. His results are parameterized by the ratio of the pressure to ionization rate. Our derived ionization rates are upper limits, but do not depend on the unknown covering factor of the clouds. If we assume the density to be 450 cm^{-3} and the temperature to be 100 K and use the ionization rate derived under these assumptions, then Draine's standard models imply steady state temperatures near 40 K for both the -47 km s^{-1} and the -39 km s^{-1} clouds, taking into account the deduced carbon depletion. Draine notes that using more recent calculations of the radiative cooling due to carbon would push the temperatures somewhat lower. However, the very high densities we derived enhance the formation rate of molecular hydrogen on grains and the heating that results as the molecules are ejected from the grains and subsequently photoionized. If the density is 450 cm^{-3}, then this enhancement will roughly double the overall heating rate, raising the temperature. Draine's standard models may also be modified to result in temperatures around 50 K by doubling the grain abundance, reducing the threshold for photoelectric emission from the grains by 25%, or halving again the carbon abundance. But 100 K seems out of reach.

On the other hand, we could consider modifying our interpretation of the data by assuming a lower temperature. As discussed above, it is possible that the departure coefficient calculations might produce a viable model that included dielectronic effects with a temperature of 50 K. Model fitting revealed the emission measure to be roughly independent of temperature and the path length l to be proportional to the temperature, implying that the electron density goes roughly as $T_e^{-1/2}$. If this is the case, then our derived densities $n_{H\,I}$ and ionization rates are also independent of temperature, and the pressures are proportional to the temperature. The carbon abundance $[N_{C^+}/N_H]$ goes as $T_e^{-1/2}$. Therefore, if the temperature were reduced, then the derived pressure would be reduced, which in Draine's (1978) models raises the temperature. The density would remain the same, maintaining the heating by molecular hydrogen formed on grains, but carbon would be somewhat less depleted, increasing the cooling efficiency. It therefore appears that the models and the data could converge at a temperature near 50 K.

To summarize the results for the higher temperature model, the carbon recombination line and H I line results might be explained self-consistently by a model consisting of diffuse H I clouds in which the temperature is $\sim$50 K, $n_{H\,I}$ is $\sim$450 cm^{-3} and n_e is $\sim$0.08 cm^{-3}, the abundance of carbon is about half the cosmic value, almost all the electrons come from ionizing all the carbon, and the hydrogen ionization rate is less than 6×10^{-17} s^{-1}. The cooling from the fine-structure transition of ionized carbon is balanced by heating from photoelectric emission from grains and from molecular hydrogen formation on grains. The two heating mechanisms contribute about equally, and each dominates the heating by cosmic rays by a factor greater than 100. The primary difference between the -47 km s^{-1} feature and the -39 km s^{-1} feature is a factor of 2 difference in the neutral hydrogen column densities.

Because the fraction of the H I seen in λ-21 cm absorption actually associated with the carbon line region is unknown in model (2), we are unable to comment on the thermal balance. It is likely that the models from Draine (1978) would not be relevant at temperatures as low as those assumed for model (2) because of the large abundance of molecular hydrogen that would be present, however.

One of the important differences between our low- and high-temperature models, discussed in the previous section, is the amount of H_2 that is present. In discussing the CO observations, Troland, Crutcher, and Heiles (1985) point out that if the H I spin temperature is in the range of our high-temperature model, 50–100 K, then the ratio $N_{H\,I}/2N_{H_2}$ is of order unity, at least in the -39 km s^{-1} feature where there does seem to be a spatial correlation between the H I and the CO. However, the spatial correlation does not mean that they are co-spatial. On the other hand, they argue that the excitation temperature of CO is, for theoretical reasons, likely to be in the 15–20 K range of our low-temperature model. It therefore appears that the choice of models to simultaneously explain the H I and recombination line observations are (*a*) a region where the temperature is $\sim$50 K and the hydrogen is perhaps half H I and half H_2 or (*b*) a region where the temperature is $\sim$16 K and the hydrogen is almost all H_2.

V. SUMMARY

We have observed recombination lines of carbon at 10 frequencies in the range 34–325 MHz in the direction of Cas A. Lines were detected at all the frequencies except near 140 MHz. The detected lines are in absorption below 115 MHz and in emission above 200 MHz.

The turnover from absorption to emission is expected from simple physical considerations based on the dominance of collisional processes at very large principal quantum numbers n and of radiative processes at lower n. The detection of an emission line in front of the strong source Cas A is direct evidence for stimulated emission of recombination lines at these frequencies. All the detected lines show two components at -47 km s^{-1} and -39 km s^{-1} which correspond to the velocities of the Perseus arm in the direction of Cas A. At 325 MHz an additional component at 0 km s^{-1}, corresponding to the Orion arm, is also detected. A carbon β line was detected at 75 MHz. The ratio of the optical depth of this line to the corresponding α line is ~ 7 which is simply the ratio of the oscillator strengths for the $\Delta n = 1$ and $\Delta n = 2$ transitions, and the broadening is consistent with α line widths at lower frequencies.

The effect of pressure broadening of recombination lines is not large in the frequency range observed here, but becomes dramatic at lower frequencies. We crudely reinterpreted the low-frequency data with the knowledge that two velocity components are present. The line broadening allows for a family of solutions in which lower temperatures allow larger electron densities: for temperatures in the range 16–100 K, the densities range from 0.4 cm^{-3} to 0.05 cm^{-3}.

We have also searched for hydrogen recombination lines at 75, 115, 220, and 325 MHz from the same clouds. No line was detected, and in our model (1) the upper limit implies hydrogen ionization rates in these clouds of $\zeta_H < 4$–6×10^{-17} s^{-1}. The combination of high pressure and low ionization rate would imply temperatures significantly lower than observed H I spin temperature in these clouds, perhaps near 50 K. Further calculations are required to demonstrate that a model with a temperature near 50 K that includes dielectronic effects, as in Walmsley and Watson (1982*b*), can fit the observed variation in line strength with frequency. A model calculated by Walmsley and Watson (1982*b*) with a temperature of 50 K and an electron density of 0.1 cm^{-3} fails to fit the observations. With the possible exception of the galactic nonthermal radiation field, the parameters for this model are quite close to those deduced from the observations in all significant respects. This high-temperature model is attractive in that it offers the possibility of a consistent physical interpretation that includes the neutral hydrogen.

The variation of the recombination line strength with frequency may be better fitted by a model with a temperature near 16 K and a density of 0.4 cm^{-3}, in which the highly excited carbon levels populations are hydrogenic. Only a fraction of the observed H I λ-21 cm optical depth can be attributed to this gas or unreasonably high densities and pressures are deduced. The ionization rate might be as high as 15×10^{-17} s^{-1} if the temperature is only 20 K.

The National Radio Astronomy Observatory is operated by the Associated Universities, Inc., under contract with the National Science Foundation. We thank an anonymous referee for bringing to our attention, the low-temperature models discussed in this paper.

REFERENCES

Anantharamaiah, K. R. 1985, *J. Ap. Astr.*, **6**, 177.
Anantharamaiah, K. R., Erickson, W. C., and Radhakrishnan, V. 1985, *Nature*, **315**, 647.
Blake, D. H., Crutcher, R. M., and Watson, W. D. 1980, *Nature*, **287**, 707.
Black, J. H., and Dalgarno, A. 1977, *Ap. J. Suppl.*, **34**, 405.
Bridle, A. H. 1969, *Nature*, **221**, 648.
Casse, J. L., and Shaver, P. A. 1977, *Astr. Ap.*, **61**, 805.
Crutcher, R. M., and Watson, W. D. 1981, *Ap. J.*, **255**, 855.
Draine, B. T. 1978, *Ap. J. Suppl.*, **36**, 595.
Ershov, A. A., Ilysov, Yu. P., Lekht, E. E., Smirnov, G. T., Solodkov, V. T., and Sorochenko, R. L. 1984, *Soviet Astr. Letters*, **10**, 348.
Ershov, A. A., Lekth, E. E., Smirnov, G. T., and Sorochenko, R. L. 1987, *Soviet Astr. Letters*, **13**, 8.
Goldberg, L. 1966, *Ap. J.*, **144**, 1225.
Goss, W. M., Kalberla, P. M. W., and Dickel, H. R. 1984, *Astr. Ap.*, **139**, 317.
Jenkins, E. B., and Shaya, E. J. 1979, *Ap. J.*, **231**, 55.
Konovalenko, A. A. 1984, *Soviet Astr. Letters*, **10**, 353.
Konovalenko, A. A., and Sodin, L. G. 1980, *Nature*, **283**, 360.
———. 1981, *Nature*, **294**, 135.
Mebold, U., and Hills, D. L. 1975, *Astr. Ap.*, **42**, 187.
Menzel, D. H. 1968, *Nature*, **218**, 756.
Payne, H. E., Salpeter, E. E., and Terzian, Y. 1983, *Ap. J.*, **272**, 540.
———. 1984, *A.J.*, **89**, 668.
Pedlar, A., Davies, R. D., Hart, L., and Shaver, P. A. 1978, *M.N.R.A.S.*, **182**, 473.
Salem, M., and Brocklehurst, M. 1979, *Ap. J. Suppl.*, **39**, 633.
Shaver, P. A. 1975, *Pramana*, **5**, 1.
———. 1976, *Astr. Ap.*, **46**, 127.
———. 1977, *Astr. Ap.*, **49**, 149.
Sorochenko, R. L., and Smirnov, G. T. 1987, *Soviet Astr. Letters*, **13**, 77.
Spitzer, L. 1978, *Physical Processes in the Interstellar Medium* (New York: Wiley).
Spitzer, L., and Jenkins, E. B. 1975, *Ann. Rev. Astr. Ap.*, **13**, 133.
Troland, T. H., Crutcher, R. M., and Heiles, C. E. 1985, *Ap. J.*, **298**, 808.
Walmsley, C. M. 1980, in *Radio Recombination Lines*, ed. P. A. Shaver (Hingham, Mass.: Reidel), p. 37.
Walmsley, C. M., and Watson, W. D. 1982*a*, *Ap. J. (Letters)*, **255**, 123.
———. 1982*b*, *Ap. J.*, **260**, 317.
Watson, W. D., Western, L. R., and Christensen, R. B. 1980, *Ap. J.*, **240**, 956.

K. R. ANANTHARAMAIAH: Raman Research Institute, Sadhashivanagar, Bangalore-560080, India

W. C. ERICKSON: Physics Department, University of Tasmania, Box 252C, GPO Hobart, Tasmania 7001, Australia

H. E. PAYNE: Space Telescope Science Institute, 3700 San Martin Drive, Baltimore, MD 21218